Aqueous Synthesis of Water-Soluble Alumoxanes: Environmentally Benign Precursors to Alumina and Aluminum-Based Ceramics

Rhonda L. Callender,[1a] C. Jeff Harlan,[1a] Noah M. Shapiro,[1a] Christopher D. Jones,[1a] Daniel L. Callahan,[1b] Mark R. Wiesner,[1c] D. Brent MacQueen,[1d] Ron Cook,[1d] and Andrew R. Barron*,[1a,b]

Department of Chemistry, Rice University, Houston, Texas 77005; Department of Mechanical Engineering and Materials Science, Rice University, Houston, Texas 77005; Department of Environmental Science and Engineering, Rice University, Houston, Texas 77005; and TDA Research, Inc., 12345 West 52nd Avenue, Wheat Ridge, Colorado 80033

Received May 16, 1997. Revised Manuscript Received August 19, 1997[⊗]

The objective of our research is the development of an environmentally benign process for the fabrication of alumina-based ceramics. We have designed an alternative synthetic pathway to alumina ceramics that does not utilize toxic reagents or volatile organic chemicals (VOCs); the aqueous synthesis of "water-soluble" carboxylate−alumoxane precursors from inexpensive boehmite feed stock. Carboxylate−alumoxanes, $[Al(O)_x(OH)_y(O_2CR)_z]_n$, were synthesized by the reaction of boehmite, $[Al(O)(OH)]_n$, with acetic acid (HO_2CCH_3), methoxyacetic acid ($HO_2CCH_2OCH_3$), (methoxyethoxy)acetic acid ($HO_2CCH_2OCH_2CH_2OCH_3$) and [(methoxyethoxy)ethoxy]acetic acid $[HO_2CCH_2(OCH_2CH_2)_2OCH_3]$. Carboxylate−alumoxanes are infinitely stable at ambient conditions in solid and solution. In addition, they show no propensity to segregation or polymerization and are readily processed in aqueous or hydrocarbon medium. Upon thermolysis the carboxylate−alumoxanes are converted to alumina. The physical and spectroscopic properties of the carboxylate−alumoxanes have been determined, including particle size, molecular weight, hardness, refractive index and dielectric constants. The application of the carboxylate−alumoxanes as preceramic binders in traditional tape casting, and infiltration agents has been demonstrated. The potential environmental impact of the new alumoxane methodology as compared to traditional approaches will be discussed.

Introduction

The oxides and hydroxides of aluminum are among the most commercially important ceramics, with a diverse range of industrial applications, including[2] precursors for the production of aluminum metal catalysts and absorbents, structural ceramic materials, reinforcing agents for plastics and rubbers, antacids, binders and absorbents for the pharmaceutical and cosmetics industries, and as low dielectric loss insulators in the electronics industry. Furthermore, ternary systems such as mullite ($Al_6Si_2O_{13}$),[3] YAG ($Y_3Al_5O_{12}$),[4] and β-alumina ($NaAl_{11}O_{17}$)[5] can offer advantages over those of the binary aluminum oxides. In addition to improved physical properties, aluminum oxides doped with an alkali, alkaline earth, transition metal, or lanthanides are of interest for catalysts, catalyst precursors, catalyst supports, and ionic conducting solids.

The environmental impact of alumina and alumina-based ceramics is in general negligible. Unfortunately, the same cannot be said for the methods of their preparation. In common with the majority of oxide ceramics, two general processes are presently employed for the tape casting fabrication of alumina green bodies: (a) the traditional ceramic powder process and (b) the solution−gelation, or "sol−gel" process. As practiced commercially, both of these processes have a significant detrimental environmental impact.

Traditional ceramic processing involves three basic steps generally referred to as powder processing, shape forming, and densification, often with a final mechanical finishing step.[6] Although several steps may be energy intensive, the most direct environmental impact arises from the shape-forming process where various binders, solvents, and other potentially toxic agents are added to form and stabilize a solid ("green") body.[7,8] The

* To whom correspondence should be addressed.

⊗ Abstract published in *Advance ACS Abstracts,* October 1, 1997.

(1) (a) Department of Chemistry, Rice University. (b) Department of Mechanical Engineering and Materials Science, Rice University. (c) Department of Environmental Science and Engineering, Rice University. (d) TDA Research, Inc.

(2) Wefers K.; Misra, C. *Oxides and Hydroxides of Aluminum*; Alcoa Laboratories: 1987.

(3) Mullite has exceptional high-temperature shock resistance and is widely used in high-temperature structural applications, see: Schneider, H.; Okada, K.; Pask, J. *Mullite and Mullite Ceramics*; Wiley: New York, 1994.

(4) Yttrium aluminum garnet (YAG) has high-temperature chemical stability and the highest creep resistance of any known oxide, leading to its evaluation as a promising fiber material for the preparation of ceramic composites; see for example: (a) King, B. H.; Halloran, J. W. *J. Am. Ceram. Soc.* **1995**, *78*, 2141. (b) King, B. H.; Liu, Y.; Basharan, S.; Laine, R.; Halloran, J. W. *Particle Sci. Technol.* **1992**, *10*, 121. (c) Morscher, G. N.; Chen, K. C.; Mazdiyasni, *Ceram. Eng. Sci., Proc.* **1994**, *15*, 181. (d) King, B. H.; Liu, Y.; Laine, R.; Halloran, J. W. *Ceram. Eng. Sci., Proc.* **1993**, *14*, 639.

(5) β-alumina or magnetoplumbite structures are being evaluated as interfacial coatings for ceramic matrix composites, see: Cinibulk, M. K. *Ceram. Eng. Sci., Proc.* **1994**, *15*, 721.

(6) See for example: (a) Kingery, W. D.; Bowen, H. K.; Uhlmann, D. R. *Introduction to Ceramics*, 2nd ed.; Wiley: New York, 1976; Chapter 1. (b) Richerson, D. W. *Modern Ceramic Engineering*; Marcel Dekker: New York, 1992; p 373.

S0897-4756(97)00368-2 CCC: $14.00

Table 1. Typical Composition of a Nonaqueous Tape-Casting Alumina Slurry[a]

function	composition	volume %
powder	alumina (Al_2O_3)	27
solvent	1,1,1-trichloroethylene/ethanol	58
deflocculent	menhaden oil	1.8
binder	poly(vinyl butyrol)	4.4
plasticizer	poly(ethylene glycol)/ octyl phthalate	8.8

[a] *Advances in Ceramics*; Vol. 9, Mangels J. A., Messing, G. L., Eds.; American Ceramic Society: Westville, OH, 1984; Vol. 9.

component chemicals listed in Table 1 (with relative percentages) are mixed to a slurry, cast, then dried and fired. In addition to any innate health risk associated with the chemical processing, these agents are subsequently removed in gaseous form by direct evaporation or pyrolysis.[9] The replacement of chlorinated solvents such as 1,1,1-trichloroethylene (TCE) must be regarded as a high priority for limiting environmental pollution.[10] The United States Environmental Protection Agency (USEPA) included TCE on its 1991 list of 17 high-priority toxic chemicals targeted for source reduction.[11] The plasticizers, binders, and alcohols used in the process present a number of potential environmental impacts associated with the release of combustion products during firing of the ceramics, and the need to recycle or discharge alcohols which, in the case of discharge to waterways, may exert high biological oxygen demands in the receiving communities.[12] It would be desirable, therefore, to be able to use aqueous processing; however, this has previously been unsuccessful due to problems associated with batching, milling, and forming.[13] Nevertheless, with a suitable choice of binders, etc., aqueous processing is possible.[14] Unfortunately, in many cast parts formed by green body processing the liquid solvent alone consists of over 50% of the initial volume, and while this is not directly of an environmental concern, the resultant shrinkage makes near net shape processing difficult. Thus, in addition to the use of environmentally benign solvents for green body processing, it would also be useful if the binder was itself a ceramic precursor. Such a system would minimize shrinkage.

Whereas the traditional sintering process is used primarily for the manufacture of dense parts, the solution−gelation (sol−gel) process has been applied industrially primarily for the production of porous materials and coatings. Sol−gel involves a four-stage process: dispersion, gelation, drying, and firing. A stable liquid dispersion or *sol* of the colloidal ceramic precursor is initially formed in a solvent with appropriate additives. By changing the concentration (aging) or pH, the dispersion is "polymerized" to form a solid dispersion or *gel*. The excess liquid is removed from this gel by drying, and the final ceramic is formed by firing the gel at higher temperatures. The common sol−gel route to aluminum oxides employs aluminum hydroxide or hydroxide-based material as the solid colloid, the second phase being water and/or an organic solvent;[15] however, the strong interactions of the freshly precipitated alumina gels with ions from the precursor solutions makes it difficult to prepare these gels in a pure form.[16] To avoid this complication, alumina gels are also prepared from the hydrolysis of aluminum alkoxides, $Al(OR)_3$ (i.e., eq 1).[17]

Table 2. Typical Composition of an Alumina Sol−Gel for Slipcast Filter Membranes

function	composition
boehmite precursor	aluminum *sec*-butoxide, $Al[OC(H)MeEt]_3$, ASB
electrolyte	HNO_3 0.07 mol/mol of ASB
complexing agent	glycerol ca. 10 wt %

$$Al(OR)_3 \xrightarrow{H_2O/H^+} \text{Al gel} \xrightarrow{\Delta} Al_2O_3 \qquad (1)$$

The exact composition of the gel in commercial systems is ordinarily proprietary; however, a typical composition will include an aluminum compound, a mineral acid, and a complexing agent to inhibit premature precipitation of the gel, e.g., Table 2.[18] The principal environmental consequences arising from the sol−gel process are those associated with the use of strong acids, plasticizers, binders, solvents, and *sec*-butanol formed during the reaction. Depending on the firing conditions, variable amounts of organic materials such as binders and plasticizers may be released as combustion products. NO_x's may also be produced in the off-gas from residual nitric acid or nitrate salts. Moreover, acids and solvents must be recycled or disposed of. Energy consumption in the process entails "upstream" environmental emissions associated with the production of that energy.

On the basis of the above discussion, it is clearly desirable to develop environmentally benign processes for the formation of alumina-based ceramic films, coatings, and bodies. In this regard we have investigated new processes that minimize chemical emissions during processing, and obviate the use of hazardous solvents and strong acids.

Carboxylate−Alumoxanes. The aluminum-based sol−gels formed during the hydrolysis of aluminum

(7) Williams, J. C. In *Treatise on Materials Science and Technology*; Wang, F. F. Y., Ed.; Academic Press: New York, 1976; p 173.
(8) Böhnlein-Mauss, J.; Sigmund, W.; Wegner, G.; Meyer, W. H.; Hessel, F.; Seitz, K.; Roosen, A. *Adv. Mater.* **1992**, *4*, 73.
(9) *Advances in Ceramics*; Vol. 9., Mangels, J. A., Messing, G. L., Eds.; American Ceramic Society: Westville, OH, 1984.
(10) Due to its widespread use as a solvent in industrial processes, TCE has become one of the most commonly found contaminants in ground and surface waters. Concentrations have been found to range from ppb to hundreds of mg. L^{-1}, see: Sawyer, C. N.; McCarty, P. L.; Parkin, G. F. *Chemistry for Environmental Engineering*; McGraw-Hill: New York, 1994.
(11) The 1988 releases of TCE reported under the voluntary right to know provisions of Superfund Amendments and Reauthorization Act (SARA) totaled 190.5 million pounds, see: LaGrega, M. D.; Buckingham, P.; L. Evans, J. C., *Hazardous Waste Management*; McGraw-Hill: New York, 1994.
(12) Thomas, R. V. *Systems Analysis and Water Quality Management*; McGraw-Hill: New York, 1972.
(13) Miller, R. E. *Am. Ceram. Soc. Bull.* **1990**, *69*, 1022.
(14) Cannon, W. R.; Becker, R.; Mikeska, K. R. *Adv. Ceram.* **1989**, *26*, 525.
(15) See for example: (a) Serna, C. J.; White, J. L.; Hem, S. L. *Soil. Sci.* **1977**, *41*, 1009. (b) Hsu P. H.; Bates, T. F. *Miner. Mag.* **1964**, *33*, 749. (c) Willstätter, R.; Kraut, H.; Erbacher, O. *Chem. Ber.* **1925**, *58*, 2448.
(16) Green R. H.; Hem, S. L., *J. Pharm. Sci.* **1974**, *63*, 635.
(17) (a) Adkins, A. *J. Am. Chem. Soc.* **1922**, *44*, 2175. (b) Teichner, S. J.; Nicolaon, G. A.; Vicarini, M. A.; Gardes, G. E. E. *Adv. Colloid Interface Sci.* **1976**, *5*, 245 and references therein. (c) Yoldas, B. E. *J. Mater. Sci.* **1975**, *10*, 1856.
(18) The aluminum compound was traditionally assumed to be the direct precursor to pseudo-boehmite. However, the gel is now known to consist of aluminum−oxygen macromolecular species with a boehmite-like core, see: Barron, A. R. *Comm. Inorg. Chem.* **1993**, *14*, 123.

compounds (a "bottom-up" synthesis) belong to a general class of compounds: alumoxanes.[19] Alumoxanes were first reported in 1958 by Andrianov[20] and were proposed to consist of linear or cyclic chains;[21−23] however, recent work from our laboratory has redefined the structural view of alumoxanes and shown that they are not chains but three-dimensional cage compounds.[24,25] For example, hydrolytically stable alumoxanes consist of an aluminum−oxygen core structure (**I**) analogous to that found in the mineral boehmite, $[Al(O)(OH)]_n$, with an organic substituted periphery.[26] On the basis of this

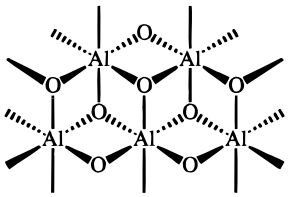

(**I**)

knowledge, we posed the question, *can alumoxanes be prepared directly from the mineral boehmite?* Applying this rational, we have developed a "top-down" approach based upon the reaction of boehmite, $[Al(O)(OH)]_n$, with carboxylic acids (eq 2).[27] Such a "top-down" approach represented a departure from the traditional synthetic methodologies.

$$[Al(O)OH)]_n \xrightarrow{HO_2CR} [Al(O)_x(OH)_y(O_2CR)_z]_n \quad (2)$$

While thermolysis of the alumoxanes yields alumina, we have shown that the carboxylate alumoxanes are readily doped with main-group, transition-metal, and lanthanide ions[28] allowing for the formation of doped and ternary aluminum oxides.[29] In addition, the physical properties, including the solubility, of these carboxylate−alumoxane are dependent on the identity of the carboxylic acid, and we have reported that water-soluble alumoxanes may be prepared by the use of polyether substitution, e.g., [(methoxyethoxy)ethoxy]acetic acid (MEEA−H).[30] However, as reported, the MEEA−alumoxane had two drawbacks with regard to its application as an environmentally benign preceramic system. First, the original samples were prepared in xylene,

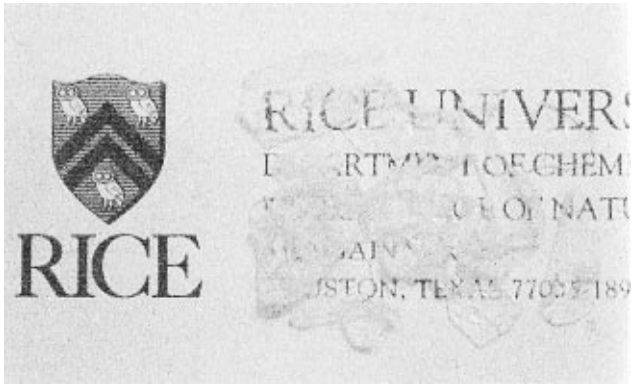

Figure 1. Photograph of MEA−alumoxane after evaporation of an aqueous solution showing its glassy appearance.

thereby nullifying their environmentally benign nature. Second, although MEEA−alumoxane was converted to alumina upon pyrolysis, the ceramic yield was relatively low (ca. 20%). It is desirable, therefore, to synthesize water soluble carboxylate−alumoxanes using water as the reaction medium and to employ smaller (low molecular weight) organic substituents to maximize the ceramic yield.[31] Furthermore, it would also be desirable to minimize the toxicity and/or environmental hazard of the organic substituents.

Prior to this present study, we have demonstrated that (a) water-soluble carboxylate−alumoxanes may be prepared,[28] (b) they are readily converted into alumina,[27] and (c) they may be doped with main-group, transition-metal, and lanthanide ions as a route to ternary aluminum-based ceramics.[28] The objectives of this present study were to (a) prepare the alumoxanes in water, (b) reduce the "organic" content of the alumoxanes and hence increase ceramic yield, (c) determine the speciation of the water-soluble alumoxanes, (d) demonstrate their use as binders in green body processing, and (e) examine their infiltration of complex shaped substrates.

Results and Discussion

Synthesis of Water-Soluble Alumoxanes. Since we have previously demonstrated that polyether-substituted alumoxanes are soluble in water[28] but desire to increase the ceramic yield, our initial studies involved the synthesis of the MEEA-substituted alumoxane in water and the synthesis of derivatives with sequential reduction in the length of the polyether chain. Thus, for the present study four different carboxylate−alumoxanes were prepared using the following: [(methoxyethoxy)ethoxy]acetic acid [$HO_2CCH_2(OCH_2CH_2)_2OCH_3$, MEEA−H, **II**], (methoxyethoxy)acetic acid [$HO_2CCH_2OCH_2CH_2OCH_3$, MEA−H, **III**], methoxyacetic acid [$HO_2CCH_2OCH_3$, MA−H, **IV**], and acetic acid [HO_2CCH_3, A−H]. For simplicity throughout this paper the following acronyms are used for the alumoxanes thus formed:

(19) The term alumoxane is commonly used to describe a species containing an oxo (O^{2-}) bridge binding (at least) two aluminum atoms, i.e., Al−O−Al.

(20) Andrianov K. A.; Zhadanov, A. A. *J. Polym. Sci.* **1958**, *30*, 513.

(21) Pasynkiewicz, S. *Polyhedron* **1990**, *9*, 429.

(22) (a) Storr, A.; Jones, K.; Laubengayer, A. W. *J. Am. Chem. Soc.* **1968**, *90*, 3173. (b) Boleslawski, M.; Pasynkiewicz, S.; Kunicki, A.; Serwatoswki, J. *J. Organomet. Chem.* **1976**, *116*, 285.

(23) Bradley, D. C.; Lorimar, J. W.; Prevedorov-Demas, C. *Can. J. Chem.* **1971**, *49*, 2310.

(24) Apblett, A. W.; Warren, A. C.; Barron, A. R. *Chem. Mater.* **1992**, *4*, 167.

(25) Landry, C. C.; Davis, J. A.; Apblett, A. W.; Barron, A. R. *J. Mater. Chem.* **1993**, *3*, 597.

(26) Alkyl-substituted alumoxanes, $[(R)Al(O)]_n$, have also been shown to consist of cage structures, in which the aluminum and oxygen are four and three coordinate, respectively, see: (a) Mason, M. R.; Smith, J. M.; Bott, S. G.; Barron, A. R. *J. Am. Chem. Soc.* **1993**, *115*, 4971. (b) Harlan, C. J.; Mason, M. R.; Barron, A. R. *Organometallics* **1994**, *13*, 2957.

(27) Landry, C. C.; Pappè, N.; Mason, M. R.; Apblett, A. W.; Tyler, A. N.; MacInnes, A. N.; Barron, A. R. *J. Mater. Chem.* **1995**, *5*, 331.

(28) Kareiva, A.; Harlan, C. J.; MacQueen, D.; B. Cook, R.; Barron, A. R. *Chem. Mater.* **1996**, *8*, 2331.

(29) Harlan, C. J.; Kareiva, A.; MacQueen, D. B.; Cook, R.; Barron, A. R. *Adv. Mater.* **1997**, *9*, 68.

(30) The use of the [(methoxyethoxy)ethoxy]acetate ligand has been shown to produce water-soluble carboxylate compounds of transition metals, see: (a) Apblett, A. W.; Long, J. C.; Walker, E. H.; Johnston, M. D.; Schmidt, K. J.; Yarwood, L. N. *Phosphorus, Sulfur Silicon* **1994**, *93−94*, 481. (b) Apblett, A. W.; Georgieva, G. D.; Reinhardt, L. E.; Walker, E. H. In *High-Temperature Synthesis of Materials*; Serio, M., Ed., American Chemical Society: Washington, DC, in press. (c) Apblett, A. W.; Breen, M. L.; Walker, E. H. *Chem. Mater.*, in press.

(31) An alternative method to enhance the ceramic yield is to lower the carboxylate:aluminum ratio in the alumoxanes.

MEEA−alumoxane ([(methoxyethoxy)ethoxy]acetate−alumoxane), MEA−alumoxane ((methoxyethoxy)acetate−alumoxane), MA−alumoxane (methoxyacetate−alumoxane), and A-alumoxane (acetate−alumoxane).

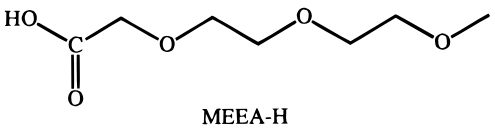

MEEA-H
(**II**)

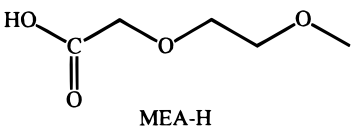

MEA-H
(**III**)

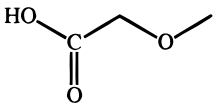

MA-H
(**IV**)

Pseudoboehmite (Catapal B Alumina, Vista Chemical Co.) and an appropriate carboxylic acid were reacted in water to yield the respective carboxylate−alumoxane; see Experimental Section. In each case the reaction produced a clear solution from which the alumoxane was isolated. As produced, the alumoxanes were each white powders; however, redissolving the powder in water and drying (50 °C) yields a glassy material suitable for storage, e.g., Figure 1. No change in composition or solubility is observed over several months under ambient conditions. Optimum reaction conditions for the ether-substituted carboxylate alumoxanes (i.e., MEEA, MEA, and MA−alumoxane) were found to require refluxing for 24−72 h (see below and Experimental Section). In contrast, refluxing acetic acid with boehmite resulted in the formation of an intractable gel and subsequently an insoluble A−alumoxane similar to the material we have described previously formed from the reaction of boehmite in neat acetic acid.[27]

As we have previously reported,[27,28] the IR spectra of all the carboxylate−alumoxanes contain bands at 1596−1586 and 1473−1466 cm^{-1}, consistent with a bridging mode of coordination (**V**) of the carboxylate to the

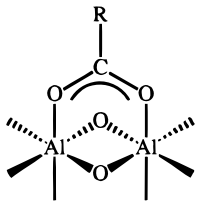

(**V**)

boehmite core.[32] Similar to the carboxylate−alumoxanes prepared in xylenes,[27,28] all IR spectra of the water-synthesized alumoxanes show broad absorption bands at 3700−3400 cm^{-1}, consistent with our previous assignment for an aluminum-bound hydroxide group. The solution ^1H and ^{13}C NMR of the carboxylate-alumoxanes indicate a single environment for the bridging carboxylates (see Experimental Section).[27] The ^{27}Al NMR spectra of the alumoxanes consist of a broad ($W_{1/2}$ = 1800−4700 Hz) resonance at ca. 6 ppm indicative of aluminum in an octahedral AlO_6 coordination environment.[33]

Scheme 1. Pictorial Representation of the Reaction of Boehmite with Carboxylic Acids[a]

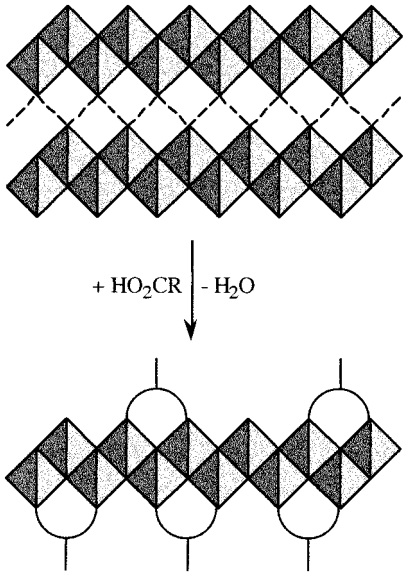

[a] The shaded triangles represent a side view of the aluminum−oxygen fused octahedra, while the carboxylate groups are represented by a semicircle and bar.[27,28]

What Are Carboxylate−Alumoxanes? We have previously proposed[27,32] that the carboxylate alumoxanes as prepared from the reaction of boehmite with carboxylic acids are formed as a consequence of the cleavage of the boehmite structure; see Scheme 1. The carboxylate groups are proposed to bind to the (100) plane of the boehmite-like core of the alumoxane. This proposal has been supported by ab initio calculations on the model compounds[34] and the isolation of a small molecular alumoxane whose structure is analogous to a boehmite-like surface.[32] However, we are interested in better understanding these water-soluble carboxylate−alumoxanes.

As noted above, the carboxylate−alumoxanes may form glassy materials by drying a water solution (Figure 1). SEM and AFM analysis demonstrate that the surface morphologies are highly dependent on the identity of the organic substituent. A SEM image of the boehmite starting material is shown in Figure 2 for comparison.

SEM analysis revealed the surface morphology of MEEA−alumoxane to be smooth with no particulates visible (Figure 3). The homogeneous nature of these films implies that they consist of an interpenetrating organic/inorganic matrix. In contrast with the MEEA−alumoxane, the surface of MEA−alumoxane appears somewhat more textured; see Figure 4. Assuming the

(32) Koide, Y. K.; Barron, A. R. *Organometallics*, **1995**, *14*, 4026.

(33) The ^{27}Al NMR resonances observed for six-coordinate aluminum centers are usually sharp ($W_{1/2}$ = 3 − 70 Hz) as is observed for $Al(acac)_3$. However, as a consequence of the multiple aluminum sites expected in carboxylate−alumoxanes, broader resonances are expected. Furthermore this effect is exacerbated by the large size of the carboxylate−alumoxanes causing slow tumbling on the NMR time scale. For a discussion of the characterization of ^{27}Al NMR spectral shifts, see: Barron, A. R. *Polyhedron* **1995**, *14*, 3197.

(34) Bethley, C. E.; Aitken, C. L.; Koide, Y.; Harlan, C. J.; Bott, S. G.; Barron, A. R. *Organometallics* **1997**, *16*, 329.

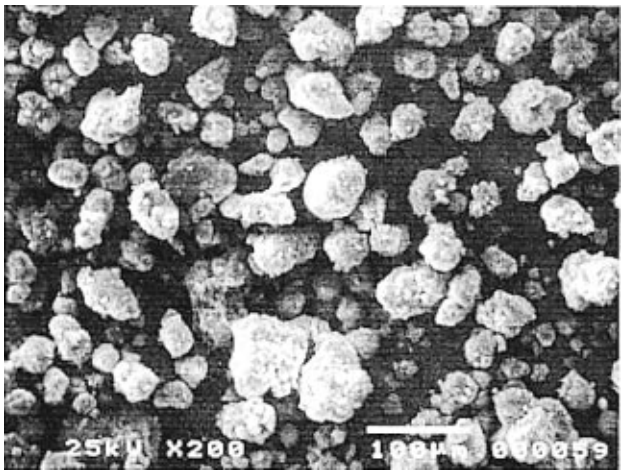

Figure 2. SEI micrograph of a sample of unreacted boehmite (catapal B alumina).

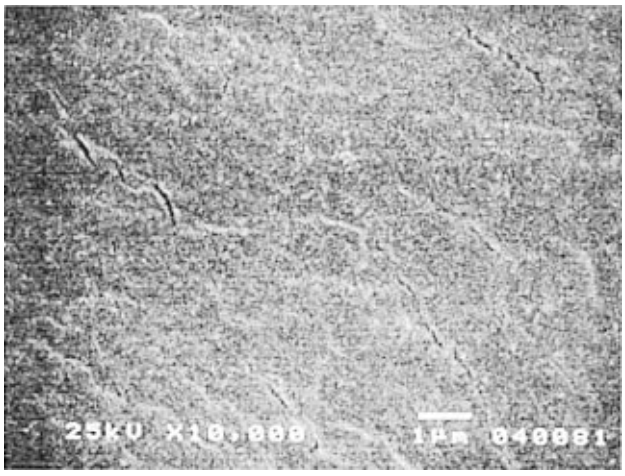

Figure 3. SEI micrograph of MEEA−alumoxane film formed by the evaporation of an aqueous solution.

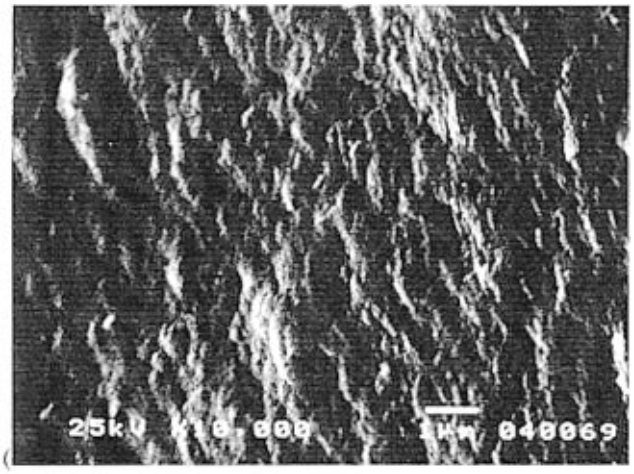

Figure 4. SEI micrograph of MEA−alumoxane film formed by the evaporation of an aqueous solution.

homogeneous nature of the surface is a consequence of the formation of an interpenetrating organic/inorganic network, this would be expected given the decrease in the organic chain length from MEEA to MEA moieties. Both SEM (Figure 4) and AFM (Figure 5a) measurements indicate that these surface features are about 200 nm in size. Higher resolution AFM analysis shows that these features are themselves textured with features in the range of 50−100 nm in size (Figure 5b).

Although MA−alumoxane appears to form a uniform glass such as MEEA−alumoxane and MEA-alumoxane, SEM indicates that the surface appearance is indicative of a colloid (Figure 6a). At higher magnification it is readily seen that the individual features of MA−alumoxane are actually fused together much like a "coral reef", while still higher magnifications (Figure 6b) reveal a cracked surface with apparent voids. The morphology of the MA−alumoxane suggests that the voids are formed as a consequence of the evaporation of water and succeeding shrinkage during dehydration. The AFM of MA−alumoxane confirms the presence of voids, but additionally indicates the relatively "smooth" areas seen in the SEM are in fact highly textured (Figure 7). As discussed in more detail below, MA−alumoxane appears to divert from many trends observed as the organic substituent length decreases in the MEEA−, MEA−, MA−, A−alumoxane series. While the A−alumoxane forms uniform bodies, SEM and AFM analysis both indicate a rough surface with features on the order of 0.1 μm in size; see Figures 8 and 9, respectively.

The AFM analyses are consistent with the "particulate" nature previously observed for the carboxylate−alumoxanes.[27] To better probe the particulate nature of the carboxylate−alumoxanes, a drop of a dilute chloroform solution of MEA−alumoxane was placed on a Si wafer and the solvent allowed to evaporate. The resulting surface was analyzed by AFM. Individual features are observed in the particle range of 100−600 nm in length (Figure 10). However, the surface texture of these particles suggests that they are actually agglomerates. This is supported by solution particle size and molecular weight measurements as discussed below.

Solution particle size measurements were performed on the carboxylate−alumoxanes by photon correlation spectroscopy (PCS) and a Coulter particle size analyzer; see Experimental Section. Figure 11 shows a graph of the particle size distribution percent by number of the MEEA−, MEA−, and A−alumoxanes in water. It can be seen from this plot that for each alumoxane a range of particle sizes is observed. The particle size number average follows the order MEEA−alumoxane > MEA−alumoxane > A−alumoxane, with the means being 67, 50, and 28 nm, respectively. Similarly, the particle size range (distribution) follows the same order, i.e., MEEA−alumoxane > MEA−alumoxane > A−alumoxane. Given that the difference in the relative length of the organic substituents is A− (estimated 2.5 Å) versus MEA− (estimated 7−8 Å) versus MEEA− (estimated 10−12 Å), the particle size variation cannot be ascribed to the chain lengths of the organic substituents since the particle size difference between the alumoxanes is significantly greater ($\Delta_{\text{particle size}} = 170-220$ Å) than the difference in substituent chain length ($\Delta_{\text{chain length}} = 2-12$ Å). Therefore, the particle size differences between each alumoxane must be due to other factors.

The particle size distribution for each of the alumoxanes is non-Gaussian, and each shows a broader range to higher particle sizes consistent with their formation via the cleavage of the significantly larger boehmite starting material (30−100 μm). This observation is in agreement with our previous proposal that the carboxylate alumoxanes are formed via the reactive cleavage

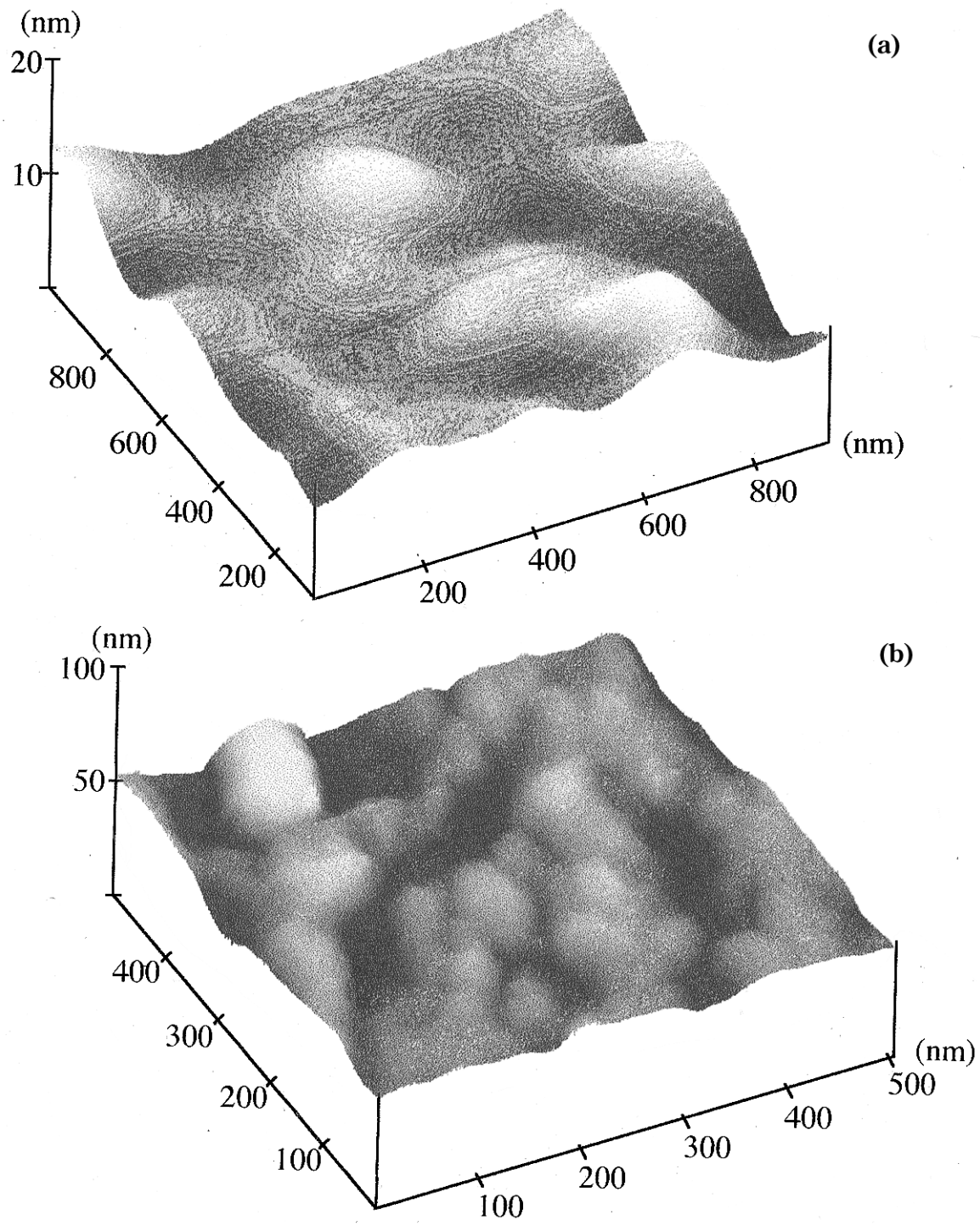

Figure 5. AFM images of MEA−alumoxane formed by the evaporation of an aqueous solution showing the textured nature of the surface.

of the boehmite precursor and its lattice; see Scheme 1.[27,32] To determine the effect of reaction time on the particle size and to obtain the reaction profile, we performed PCS analyses on aliquots taken from a reaction flask of MEA−H and boehmite in aqueous solution. The results of this study are shown in Figure 12. On the basis of the PCS data, it would appear that the 30−100 μm sized particles of boehmite are indeed rapidly cleaved to yield a broad distribution of alumoxane sizes. Upon further reaction the distribution appears to decrease significantly in width with only a small change in the average particle size. This suggests that small pieces are successively broken off the large boehmite substrate, rather than a large piece being cleaved in half, and the halves being halved, etc. It should be noted that the Coulter particle size analyzer employed (see Experimental Section) does not allow for the accurate measurements below ca. 5 nm thus precluding the determination as to whether smaller alumoxanes are formed over extended reaction times.

The time dependence of the reaction of MEA−H with boehmite and the particle size results shown in Figures 11 and 12 suggest that the reaction rate is highly dependent on the identity of the carboxylic acid. It should be noted that for any particular carboxylate−alumoxane with particle sizes below ca. 100 nm the ceramic yield appears to be invariant or the variation is not especially sensitive. The particle size, however,

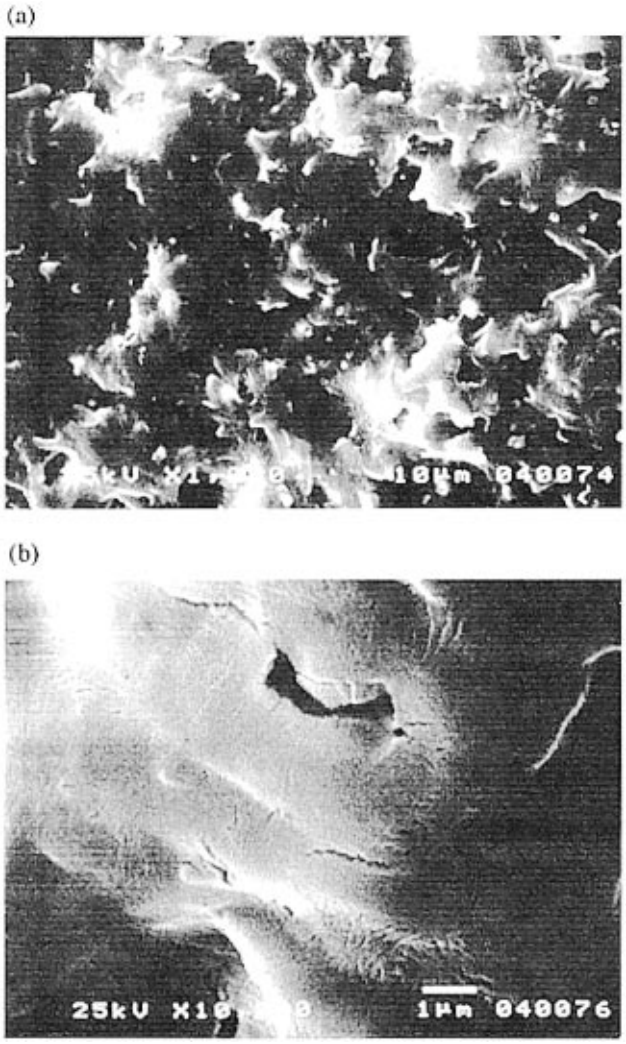

Figure 6. SEI micrographs of MA−alumoxane film formed by the evaporation of an aqueous solution, showing the coral reef-like surface

has a significant bearing on the processability and physical properties of the alumoxanes.

The PCS results for MA−alumoxane are very different from MEEA−, MEA−, and A−alumoxanes. The data indicate that the MA−alumoxane, formed under reaction conditions similar to those employed for MEEA− and MEA−alumoxanes, consists of large (200−1400 nm) sized particles (Figure 13). Furthermore, there is a distinct bimodal distribution. These data are consistent with our observations for the MA-alumoxane as being distinct from the other carboxylate−alumoxanes studied herein. On the basis of the results of the particle size versus reaction time analyses (Figure 12) we propose that the reaction time (24 h.) employed for the MA−alumoxane results in incomplete reaction. Unfortunately, extended reaction times result in gelation and preclude successful isolation.

Gel permeation chromatography (GPC) is commonly used for the determination of molecular weights of polymers as distinct from particle size. Figure 14 shows the GPC results in HFIPA [$HOC(H)(CF_3)_2$] for the samples of MEEA−alumoxane (Figure 14a), MEA−alumoxane (Figure 14b), and MA−alumoxane (Figure 14c), studied by PCS above. Consistent with the PCS data the MEEA− and MEA−alumoxanes have an average molecular weight (M_w) of 20 100 and 17 400 amu, respectively, while the MA−alumoxane shows a much higher M_w of 140 000 amu. However, although the M_w/M_n for MA−alumoxane is relatively narrow (1.54), those for the MEEA (4.10) and MEA (3.54) homologues are significantly increased due to a trimodal molecular weight distribution. This effect was not discernible from PCS data, and it is possible that this difference is related to the solvents employed. It is conceivable that interparticle agglomeration is assisted by hydrogen bonding in aqueous solution where such effects are minimized in the HFIPA used for GPC measurements.

On the basis of the spectroscopic characterization, the carboxylate−alumoxanes are best considered to be nanoparticles of aluminum oxide hydroxide (or boehmite) which are capped with carboxylate residues. In this regard they may be regarded as analogues of the capped TiO_2 nanoparticles prepared by the hydrolysis of ethanolic solutions of $Ti(OEt)_4$.[35]

Properties of Carboxylate Alumoxanes. Although the main thrust of the present work is to develop environmentally benign precursors for aluminum-based ceramics, we have an interest in the application of the alumoxanes as inorganic−organic hybrid materials. Therefore, we have investigated the physical properties of the alumoxanes.

The physical appearance, solubility, and surface morphology of the carboxylate−alumoxanes are dependent on the identity of the carboxylate substituent. Thus, MEEA−A and MEA−A are white crystalline powders which readily dissolve in water to form clear glassy materials (see Figure 15). In addition, they are soluble in methylene chloride, chloroform, and ethanol, which facilitates spectroscopic characterization. MA−alumoxane is a white solid which dissolves in water sparingly and is only slightly soluble in methanol. Similarly, A−alumoxane is soluble in water and methanol. The alumoxanes are indefinitely stable under ambient conditions and are adaptable to a wide range of processing techniques, including infiltration (see below), dip-coating, spin-coating, and spray-coating onto various substrates. Concentrated mixtures of the alumoxanes with water form rigid gels (Figure 16).

The carboxylate−alumoxanes are apparently soluble in water, in which they make clear free-flowing solutions. However, given the particle sizes measured (ca. 5−1400 nm), it may be more appropriate to consider the carboxylate−alumoxanes in aqueous solution to be colloidal dispersions.[36] While concentrated water dispersions show a well-defined Tyndall effect (i.e., they scatter an incident light beam) typical of a colloidal suspension, mixtures in chloroform and dilute mixtures in water do not. This suggests that the carboxylate−alumoxanes border between colloid and true solution. It is interesting to ask the question, *why do these carboxylate−alumoxanes form such good (homogeneous) dispersions in water?* In the case of the polyether substituted derivatives it is reasonable to propose that solubilization occurs through significant hydrogen-bonding interactions with the oxygens in the chain (Figure

(35) Barringer, E. A.; Bowen, H. K. *Langmuir* **1985**, *1*, 414 and references therein.

(36) A colloid is made up of particles of one substance dispersed throught another. The particles of the dispersed substance range in diameter from 1 nm to 1 μm.

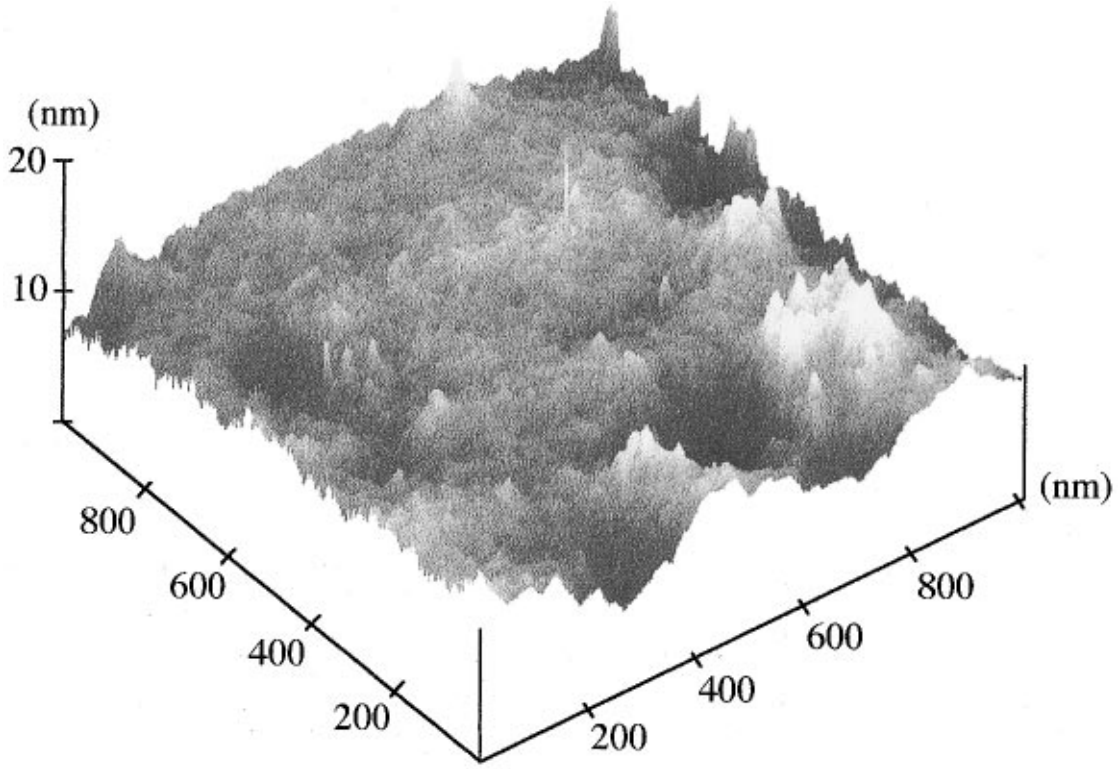

Figure 7. AFM of MA−alumoxane showing the presence of voids (ca. 0.2 μm in diameter) within the textured surface.

17a). Supporting evidence for this proposal is the molecular structure of $Ca[(O_2CCH_2CH_2OCH_2CH_2)_2O]\cdot 2H_2O$ in which the waters are hydrogen bonded to the polyether-substituted ligand.[37] Similar effects have been observed in the solubility of polymers.[38] Clearly these effects cannot explain the miscibility of A−alumoxane with the acetate substituent. While we have no direct evidence, it is possible that the water solubilization arises from hydrogen-bonding interactions with the alumoxane core; see Figure 17b.

The relative solubility of the carboxylate−alumoxanes will affect the way in which they can be manipulated. In particular, the amount of the carboxylate−alumoxane required to form a rigid gel (Figure 16) is expected to greatly depend on the organic substituent. It may be contemplated that the longer the polyether chain, the greater the potential for hydrogen bonding and thus the greater the solubility/miscibility in water. However, as is shown in Table 3, this is not entirely the case. It would appear that up until MEA−alumoxane this trend is observed, excepting MEA−alumoxane, which shows a greater solubility in water than MEEA−alumoxane.[39] We have observed a similar effect for the solubility of straight-chain hydrocarbon-substituted carboxylate alumoxanes in aromatic solvents. Carboxylate−alumoxanes $[Al(O)_x(OH)_y(O_2CR)_z]$ ($R = C_nH_{2n+1}$) with $n \leq 5$ are insoluble, $n = 6, 7, 8$ are soluble, and $n \geq 9$ are again insoluble.

To determine the potential of the alumoxanes for optical coating applications, we have determined the optical transparency and refractive index of the alumoxanes. The UV−visible spectrum of each of the

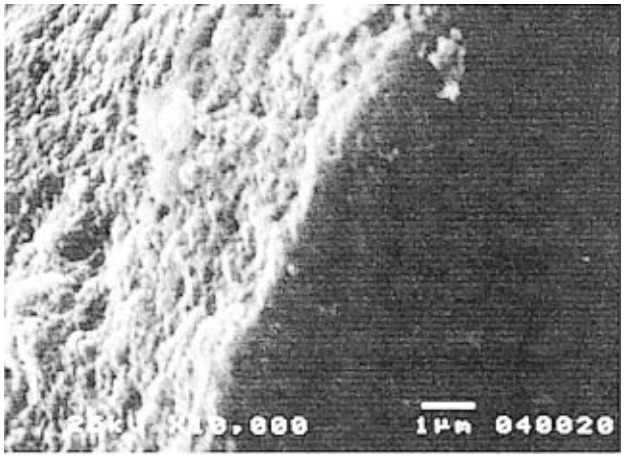

Figure 8. SEI micrographs of A−alumoxane film formed by the evaporation of an aqueous solution.

polyether substituted carboxylate−alumoxanes shows an absorption at 195−198 nm: MEEA−alumoxane (195 nm, $\epsilon = 440$), MEA−alumoxane (196 nm, $\epsilon = 851$), MA−alumoxane (198 nm, $\epsilon = 902$).[40] In contrast, the A−alumoxane shows no appreciable absorption above 190 nm. However, the presence of metal dopants can be used to modify the UV−visible characteristics. For example, reaction of MEEA−alumoxane with $Fe(acac)_3$ results in a facile transmetalation (eq 3) and the

$$[Al(O)_x(OH)_y(O_2CR)_z] + nFe(acac)_3 \rightarrow [Al_{1-n}Fe_n(O)_x(OH)_y(O_2CR)_z] + nAl(acac)_3 \quad (3)$$

formation of Fe-doped MEEA−alumoxane. The UV−visible spectra of which is consistent with Fe^{3+} in the

(37) Hanusa, T., private communication.
(38) Hariharan, R. Thesis, Princeton University, 1996.
(39) The observed "solubility" of the alumoxanes in water appears to be independent of the ceramic yield, i.e., the solubility is not dependent on the relative number of carboxylate groups per aluminum.

(40) Molar extinction coefficients have the units 1000 cm^2 (mol of Al)$^{-1}$.

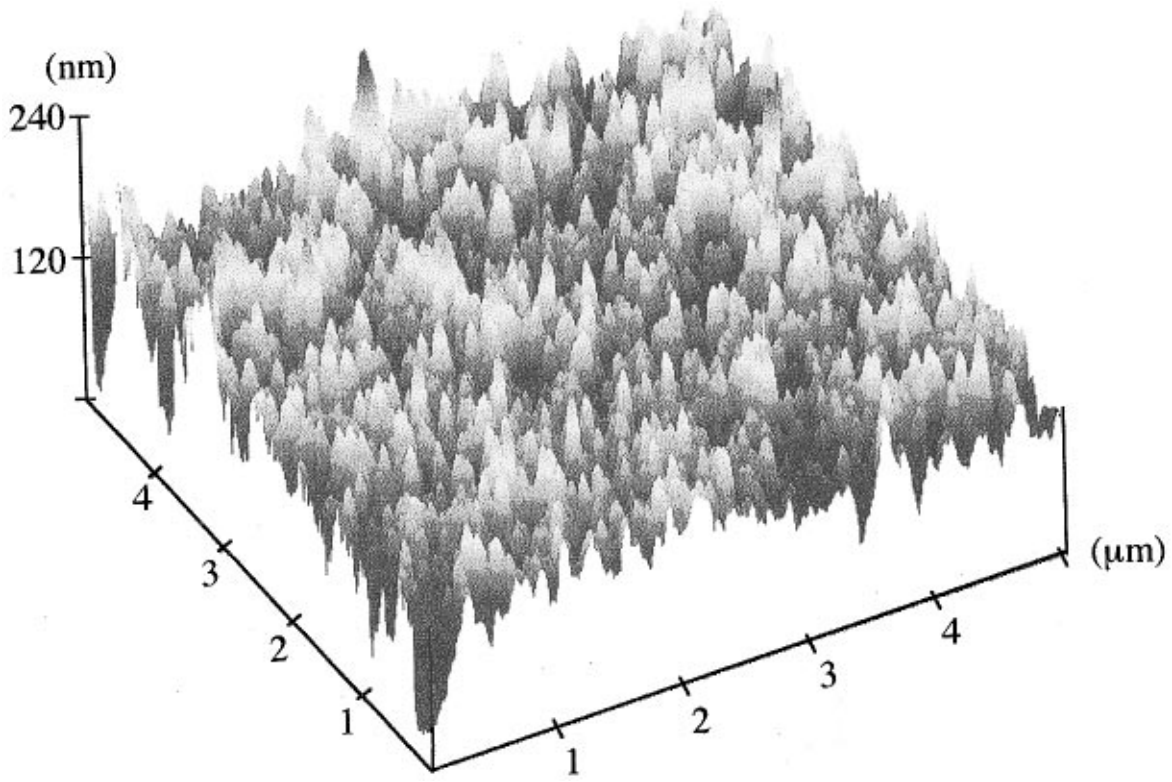

Figure 9. AFM image of A−alumoxane formed by the evaporation of an aqueous solution showing the textured nature of the surface.

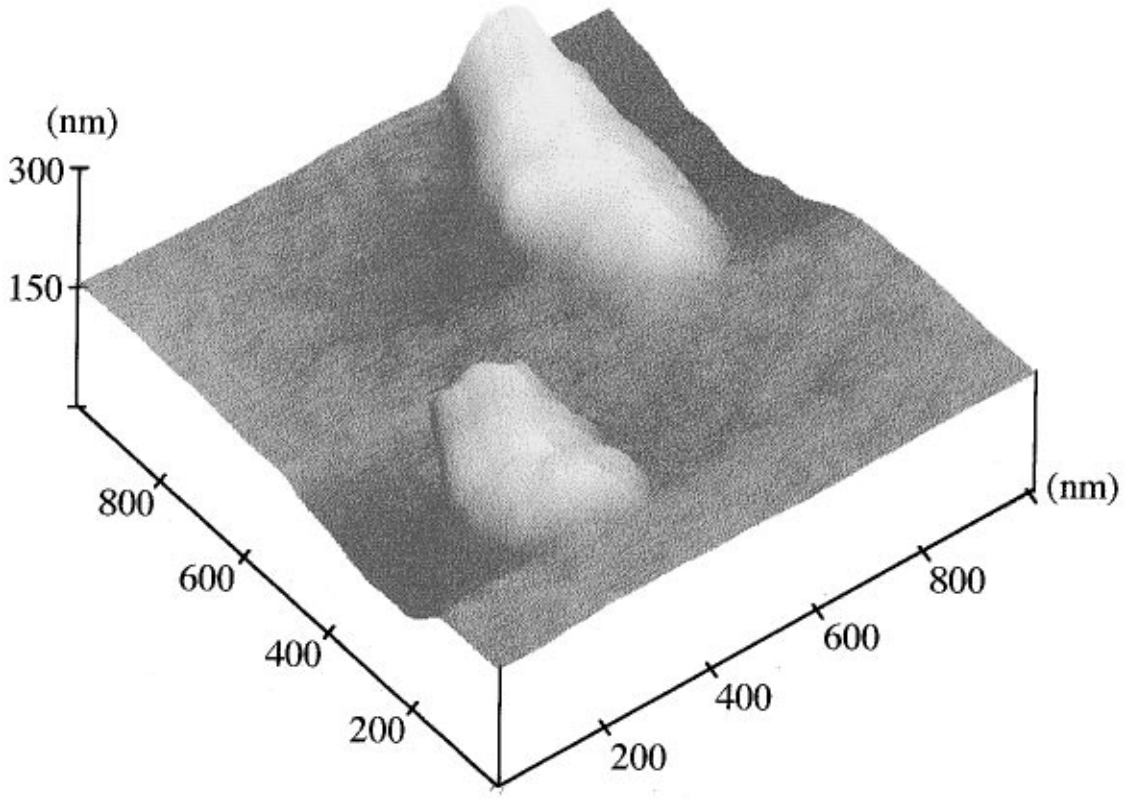

Figure 10. AFM image of a particle of MEA−alumoxane on a silicon wafer surface. Note: The apparent dip in the Si wafer around the alumoxanes is an artifact due to the height difference of the alumoxane particle and the silicon.

octahedral lattice sites of the alumoxane's boehmite-like core (Figure 18).

The refractive indexes (n_D) of the carboxylate alumoxanes measured at $\lambda = 632.8$ nm are in the range 1.4−1.6 (Table 3), intermediate between that of boehmite (1.62) and the organic substituents; acetic acid (1.3) and glycol (1.4).[41]

(41) It should be noted that catapal B alumina contains ca. 0.2% TiO_2 and 0.4% carbon.

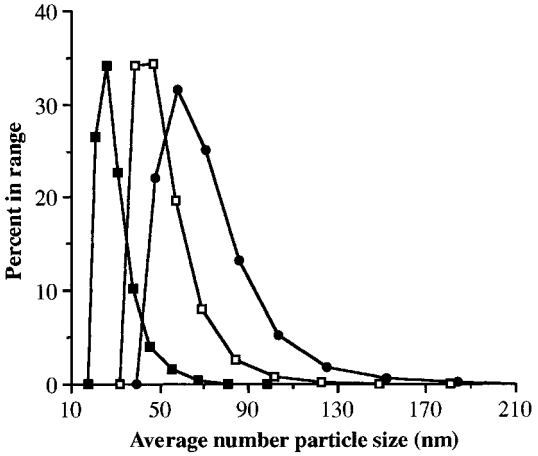

Figure 11. Plot of particle size distribution, determined by photon correlation spectroscopy (PCS), of the MEEA−, MEA−, and A−alumoxanes in water.

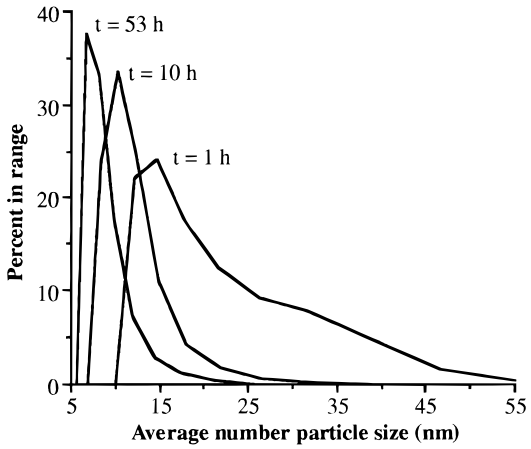

Figure 12. Plot of particle size distribution, determined by photon correlation spectroscopy (PCS), of MEA−alumoxane for various aliquots removed from the reaction of MEA−H with boehmite.

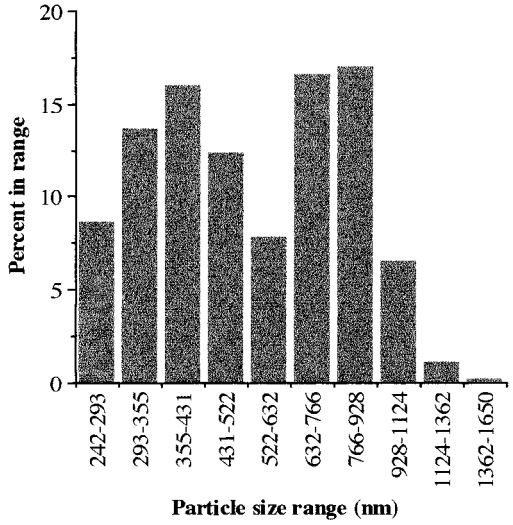

Figure 13. Bar graph showing the particle size distribution as determined by photon correlation spectroscopy (PCS) of MA−alumoxane.

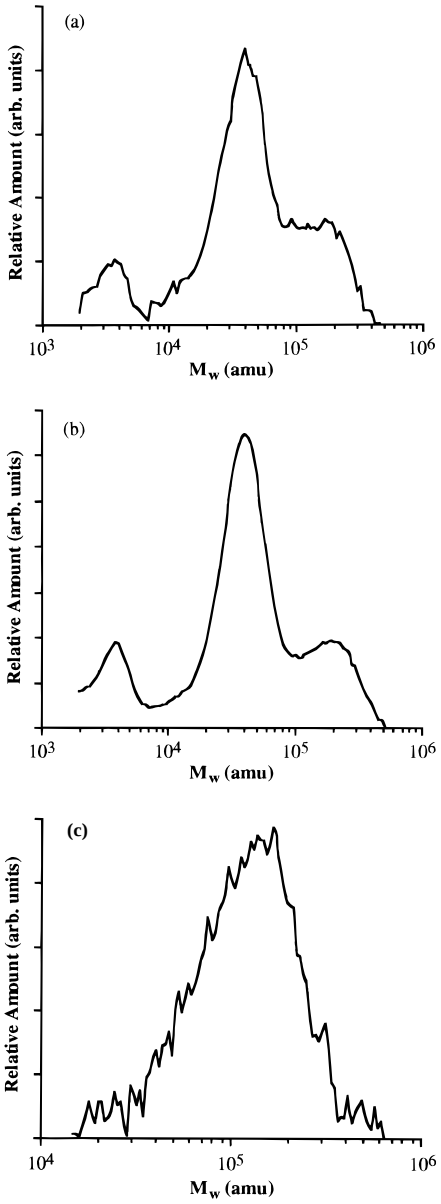

Figure 14. GPC results for samples of (a) MEEA−alumoxane, (b) MEA−alumoxane, and (c) MA−alumoxane.

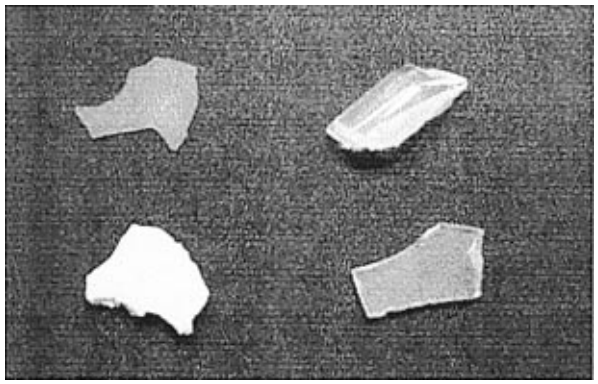

Figure 15. Photograph of carboxylate−alumoxanes showing their appearance after evaporation from aqueous solution. MEEA−alumoxane (lower right), MEA−alumoxane (upper right), MA−alumoxane (lower left), and A−alumoxane (upper left).

The dielectric constant (ϵ) of the carboxylate−alumoxanes were measured at 10^3 Hz; see Table 3. The values of 1.5−1.7 are significantly lower than that of alumina (4.5−8.4 at 10^6 Hz) and close to that of polyethylene (2.37 at 10^3 Hz), suggesting that the electronic properties are dominated by the organic part of the alumoxane. Similarly, the hardness of the carboxylate alumoxanes (Table 3), while dependent on the organic substituents, is comparable to organic rather

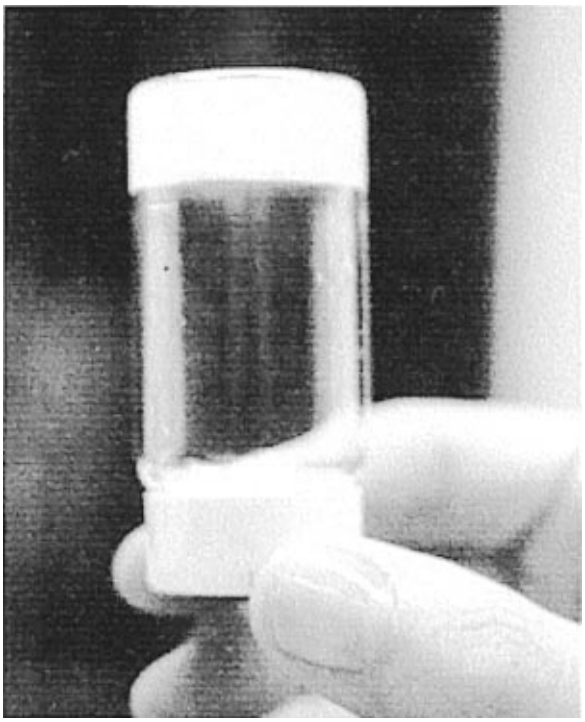

Figure 16. Sample of a rigid gel formed from MEEA−alumoxane (0.3 g) in water (1 mL).

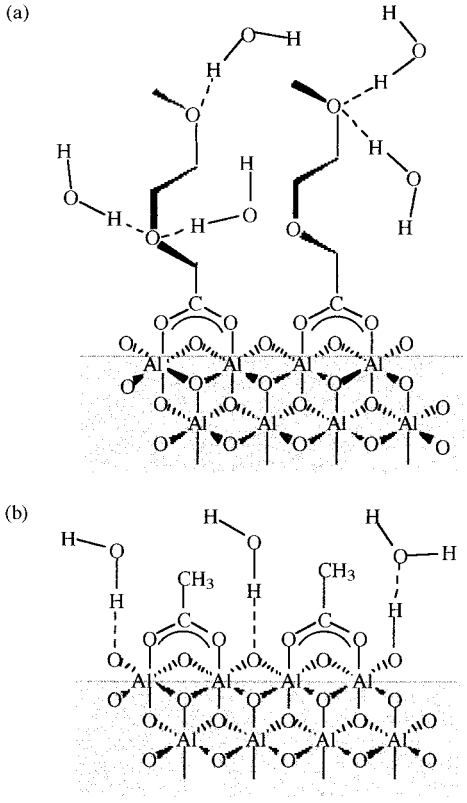

Figure 17. Schematic representation of the solubilization of the alumoxanes with (a) MEEA, MEA, and MA substituents and (b) acetate. The shaded area represents the surface of the alumoxane particle.

than inorganic materials.

Conversion of Carboxylate−Alumoxanes to Alumina. Thermogravimetric/differential thermal analysis (TG/DTA) of the carboxylate−alumoxanes generally indicates two major decomposition regions as can be seen from the representative TG/DTA of MEEA−alumoxane shown in Figure 19. The relative mass loss and temperatures at which these regions occur is dependent on the identity of the carboxylic acid. We have previously shown[25] that the volatiles are predominantly the acid and water with traces of the ketone, i.e., acetone is liberated from the A−alumoxane. As may be expected, the ceramic yield is conditional on the identity of the carboxylic acid: greatest for A−A (ca. 75%), lowest for MEEA−A (ca. 20%); see Table 3. Representative SEM and AFM images of the surface of α-Al_2O_3 formed from A−alumoxane are shown in Figures 20 and 21, respectively. These should be compared to the before-firing sample shown in Figures 8 and 9.

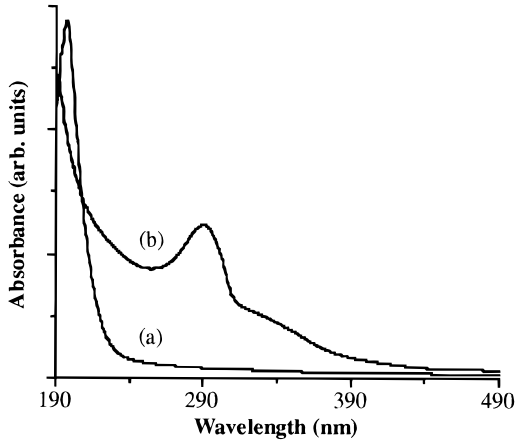

Figure 18. UV−visible spectra of (a) MEEA−alumoxane (195 nm, $\epsilon = 440$) and (b) Fe-doped MEEA−alumoxane (191 nm, $\epsilon = 760$; 290 nm, $\epsilon = 377$).

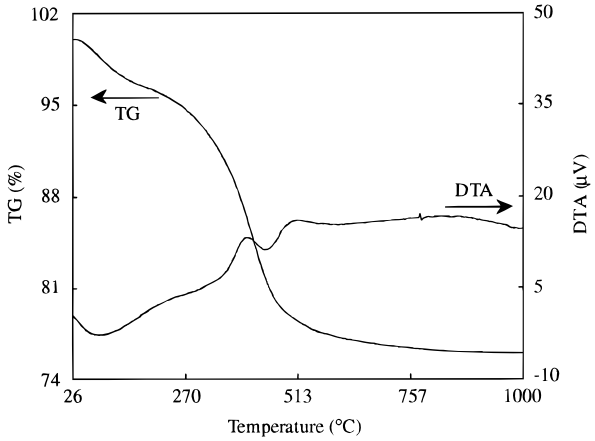

Figure 19. Representative thermogravimetric/differential thermal analysis (TG/DTA) of MEEA−alumoxane.

All of the carboxylate−alumoxanes decompose above 180 °C to give amorphous alumina (Table 3). Firing above 900 °C (≥3 h) results in the formation of better ordered mixed phase γ-Al_2O_3 (JCPDS 29-63) and α-Al_2O_3 (Corundum, JCPDS 42-1468), as would be expected based on the known transformation sequence of aluminas.[2] All of the carboxylate alumoxanes are converted to α-alumina above 1200 °C with firing times ≥4 h.[42] It is interesting to note that the A−alumoxane is highly reactive and forms crystalline α-Al_2O_3 at temperatures below 1200 °C (1170 °C). The lower temperature of this phase formation and failure to observe γ-Al_2O_3 from A−alumoxane is consistent with the very small inital

(42) No carbon is detected in the resulting ceramic if an oxidizing atmosphere is employed.

Table 3. Selected Physical Properties of the Carboxylate−Alumoxanes

alumoxane	gel point in water (g mL^{-1})[a]	refractive indexes (n_D)	dielectric constant (ϵ)	hardness V_H[d] (kg mm^2)	dec temp[f] (°C)	ceramic yield (%)
MEEA−alumoxane	0.30	1.5	2.7	2−40	142/370	20
MEA−alumoxane	0.95	1.5	2.5	20−40	160/370	27
MA−alumoxane	0.11	*b*	*c*	>40[e]	230/360	30
A−alumoxane	0.20	1.5	2.5	90	155/520	76

[a] Defined as the mass of alumoxane required to form a solid gel in 1.0 mL of water. [b] Sample too opaque. [c] Inconsistent data. [d] Vickers hardness. [e] Sample too brittle for acurate measurement. [f] Temperatures at which alumoxane starts to decompose and at which decomposition is complete.

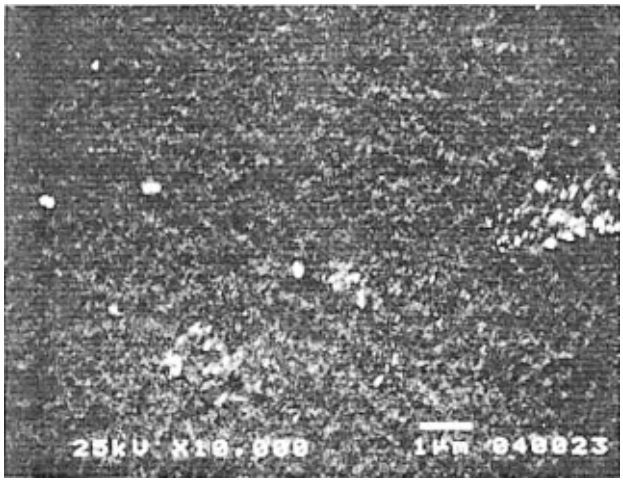

Figure 20. SEM of α-Al_2O_3 surface formed by the pyrolysis of A−alumoxane at 1000 °C for 6 h. This should be compared to the unfired sample in Figure 8.

pore size (large surface area) and rapid sintering rates.

All four alumoxanes produced uniform, translucent fired bodies with differences in microscopic porosity but similarities in macroscopic density. Both MEEA− and MEA−alumoxane produce either high porosity translucent solid "foam" or slightly translucent bodies consistent with a smaller porosity/higher microscopic density. However, the macroscopic densities are very similar, i.e., $\rho \approx 2.2-2.5$ g mL^{-1}. MA− and A−alumoxane were apparently dense white solids (e.g., Figure 15), the former exhibiting some translucence consistent with its higher density (MA−alumoxane, $\rho \approx 3.4$ g mL^{-1}; A−alumoxane, $\rho \approx 2.6$ g mL^{-1}).

The α-Al_2O_3 formed from MEEA−alumoxane exists as a nanocrystalline matrix with a very high volume of large interconnecting pores as determined by TEM studies. In contrast, analysis of the α-Al_2O_3 formed from A−alumoxane revealed very fine uniform intragranular porosity. Although the crystalline size is quite large in these samples, the detailed intragranular structure suggests a previous nanocrystalline structure. We propose that initial firing gives rise to a transition phase of porous nanocrystalline γ-Al_2O_3 which is converted to α-Al_2O_3 and undergoes subsequent growth around the initial pore structure with no or little additional densification. The difference in pore size and structure is most consistent with the known change in ceramic yield, i.e., a higher organic volume outgassed produces larger pores. Using the alumoxane series, it should be possible to engineer pore size continuously between these extremes by using mixed ligand solutions. Detailed TEM studies will be reported elsewhere.[43]

As noted in the Introduction, we have previously reported that the carboxylate−alumoxanes may be used as precursors to ternary and doped alumina ceramics.[28] Reaction of the carboxylate−alumoxane with a metal acetylacetonate complex, M(acac)$_n$ (**VI**), results in trans-

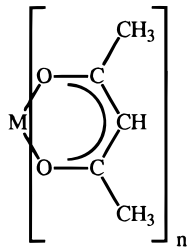

(**VI**)

metalation and the formation of a doped-alumoxane. Upon thermolysis these doped alumoxanes result in homogeneous mixed-metal oxides. We have repeated this process with the alumoxanes prepared in water with Ca(acac)$_2$, Y(acac)$_3$, and Mn(acac)$_2$ for the formation of hibbonite, YAG,[29] and Mn-doped Al_2O_3,[44] respectively. The doped alumoxanes were prepared by mixing aqueous solutions of a carboxylate−alumoxane and the appropriate metal precursor compound. No difference was observed between these alumoxanes and those we have previously reported.[28]

Application of the Alumoxanes as Binders for Green Bodies. As discussed in the Introduction, traditional ceramic processing involves three basic steps generally referred to as powder processing, shape forming, and densification, often with a final mechanical finishing step.[7] Unfortunately, this process inherently results in significant shrinkage during processing, since a ceramic powder is mixed with various binders, solvents, and other agents to form and stabilize a solid ("green") body.[8] These agents are subsequently removed as gaseous products by direct evaporation or pyrolysis. In many cast parts, the liquid solvent alone consists of over 50% of the initial volume of material. These issues could be mitigated to a great extent if a single species could be employed as a binder that is itself converted to a ceramic. If the extent of shrinkage could be limited to acceptable values, near-net shape fabrication of ceramic bodies could also be achieved. Furthermore, the green strength of the ceramic plays an important role in ceramic processing. Our approach involves the application of processable alumoxanes that are converted into alumina-based ceramics by firing.

Using wax molds, we have been able to prepare shaped green bodies with 70 wt % solutions of alumina

(43) Callahan, D. L; Callender, R. L.; Barron, A. R., submitted for publication.

(44) Cook, R. L.; Wang, C.; Harlan, C. J.; Kareiva, A.; Barron, A. R. *Mater. Res. Soc., Symp. Proc.*, in press.

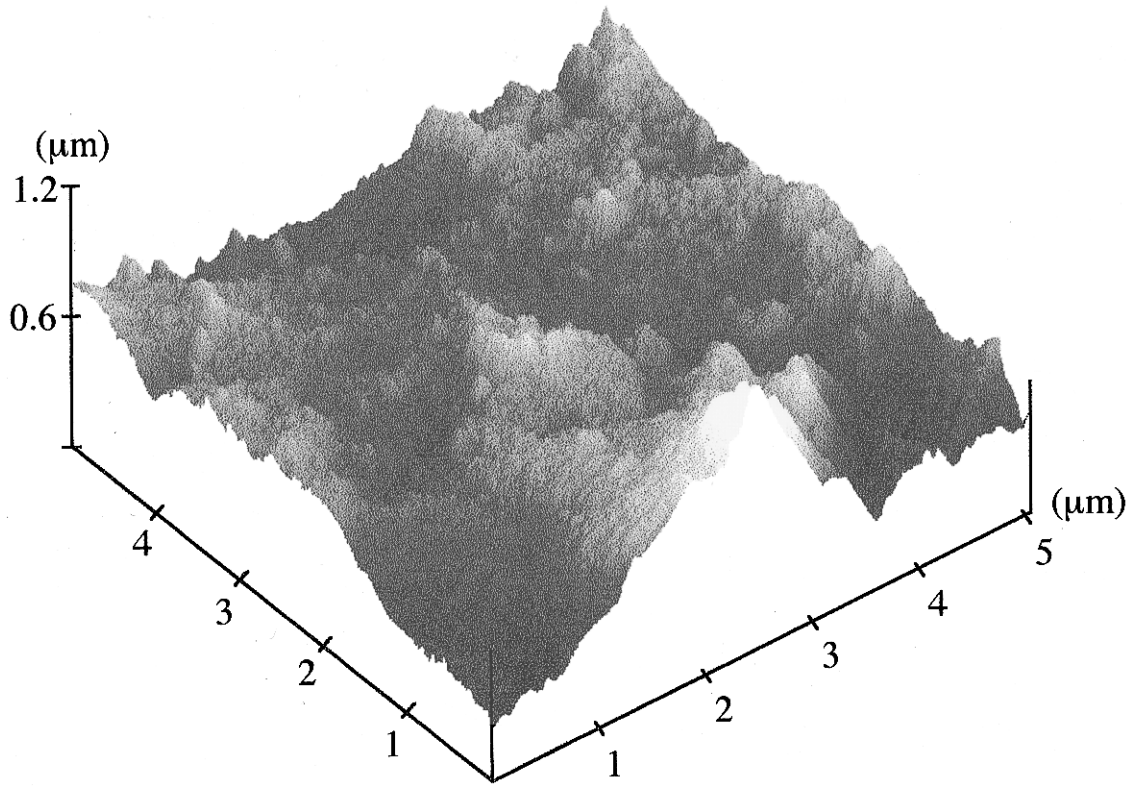

Figure 21. AFM of α-Al_2O_3 surface formed by the pyrolysis of A-alumoxane at 1000 °C for 6 h. This should be compared to the unfired sample in Figure 9.

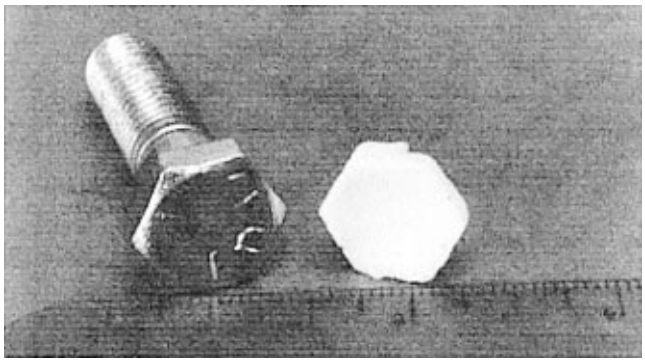

Figure 22. Photograph of a hexagonal bolt used to make a wax mold (left) and the alumoxane:alumina green body thus formed (right).

and the water-soluble alumoxane (Coors, 99.5% Al_2O_3) powder in a 1:2 mixture. These mixtures were pourable, and thus the alumoxane acts as both the transport media (solvent) and the binder. The material can be cast into a wax mold and dried. After removal of the wax by melting, the green bodies were set (120 °C for 5 h). The setting occurred without any addition of cross-linking agents. Calcination results in the formation of an alumina-shaped body with less than 6% shrinkage in going from green to fired material. An example of a simple hexagonal bolt is shown in Figure 22. SEM images of the surface of a similarly prepared body is shown in Figure 23.

The above results demonstrate that the carboxylate alumoxanes are suitable to be used as the binder in green body processing and allow for a significant reduction in shrinkage since the "binder" is itself a precursor for the ceramic. This process is shown schematically in Figure 24. An additional advantage of the alumoxane binder route is that doped alumoxanes may be used so that ceramic matrix composites (CMCs) are readily produced in which the matrix and reinforcement phases are different. However, it is necessary to have no more than 40% loading of a 50% ceramic yield binder to obtain dense ceramic CMCs.

Infiltration of Alumoxane Slips into Porous Substrates. In addition to the significant shrinkage observed during sintering of a green body, there is often undesirable porosity in the finished ceramic body. This effect is exacerbated in the case of ceramic fiber−ceramic matrix composites in which the back stress between the reinforcing phase (fiber) and the matrix results in resistance to densification (i.e., significant porosity). A second problem with ceramic composites processed through traditional routes is that the surface is frequently rough. This occurs from both the sintering step, as well as physical handling and postsintering machining. As indicated above a possible solution to these effects is the use of the alumoxanes as a preceramic binder (see above). However, an alternative is to postprocess infiltrate the alumoxane solution (or slip) into the porous ceramic. Sintering of this material will cause infiltration of the original ceramic by a second ceramic material. Clearly, this can be of the same phase or designed to enhance reinforcing phase (fiber) and the matrix interactions. It is important to note that PCS and GPC measurements indicate that the alumoxanes may be selectively prepared with a particle size of 5−150 nm. Thus, it is possible that pores in this range may readily be completely infiltrated, rather than just blocked at the surface. To ascertain whether the alumoxane will infiltrate (and wet) complex shapes such as fiber tows or the voids that exist in a preformed body, we have studied the infiltration and heat treatment of

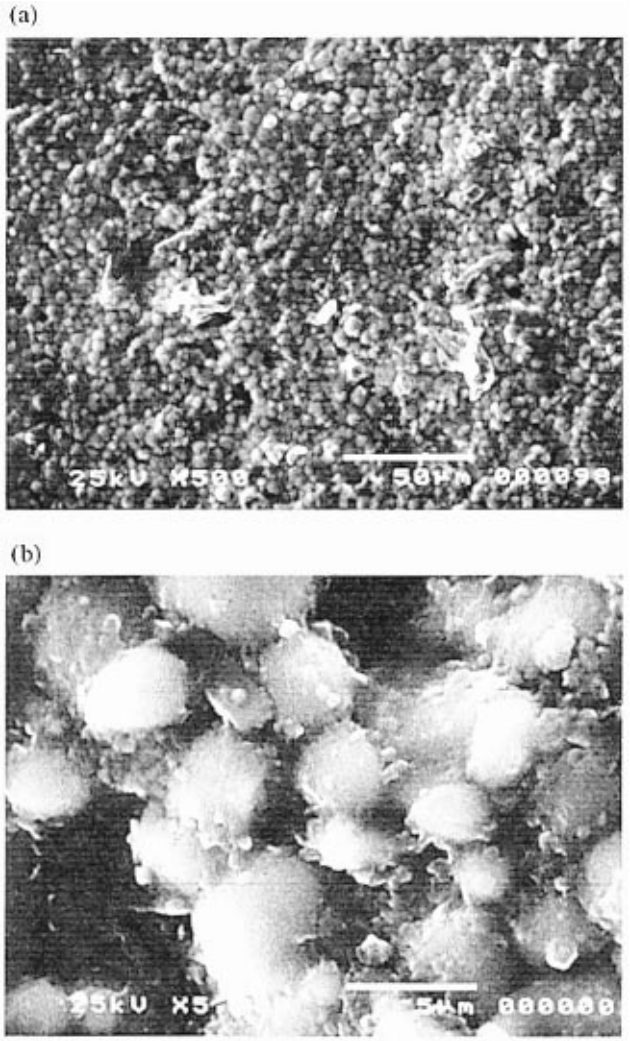

Figure 23. SEM image of the surface of an alumina disk prepared from an alumina/MEEA−alumoxane green body sintered at 1000 °C for 16 h.

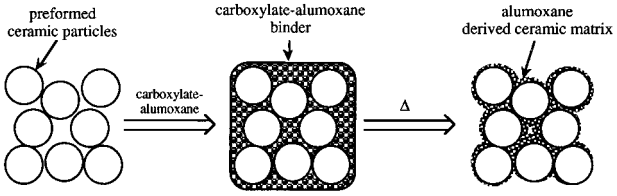

Figure 24. Schematic representation of the application of the carboxylate−alumoxanes as binder/plastisizer in green body processing.

a cellulose fuel filter and a coarse porosity glass filter frit.

An automotive fuel filter was impregnated with MEEA−alumoxane (see Experimental Section) and heated to 1000 °C in air to burn out all the organic residues. Due to the relatively low processing temperature, the resultant alumina "filter" had very little strength; however, as can be seen from Figure 25, the macroscopic shape of the filter was retained. Previous SEM analysis of similar paper substrates demonstrated that the alumina ceramic formed upon oxidative thermolysis retains the structure of the paper fibers with little evidence for particulate oxide residues.[28]

As a further example, a coarse glass filter frit (pore size "C") was infiltrated with an aqueous solution of MEA−alumoxane. Organic burnout and dehydration

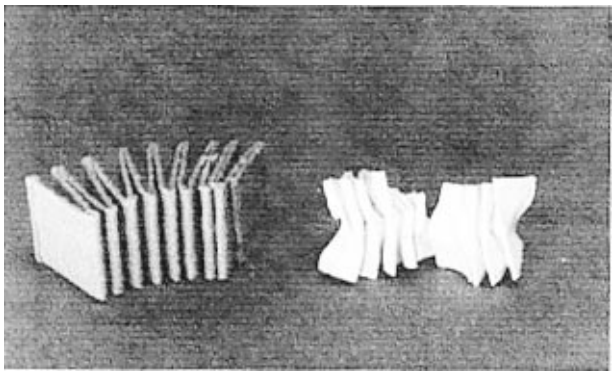

Figure 25. Comparison of paper fuel filter (left) and the ceramic form after calcination (right).

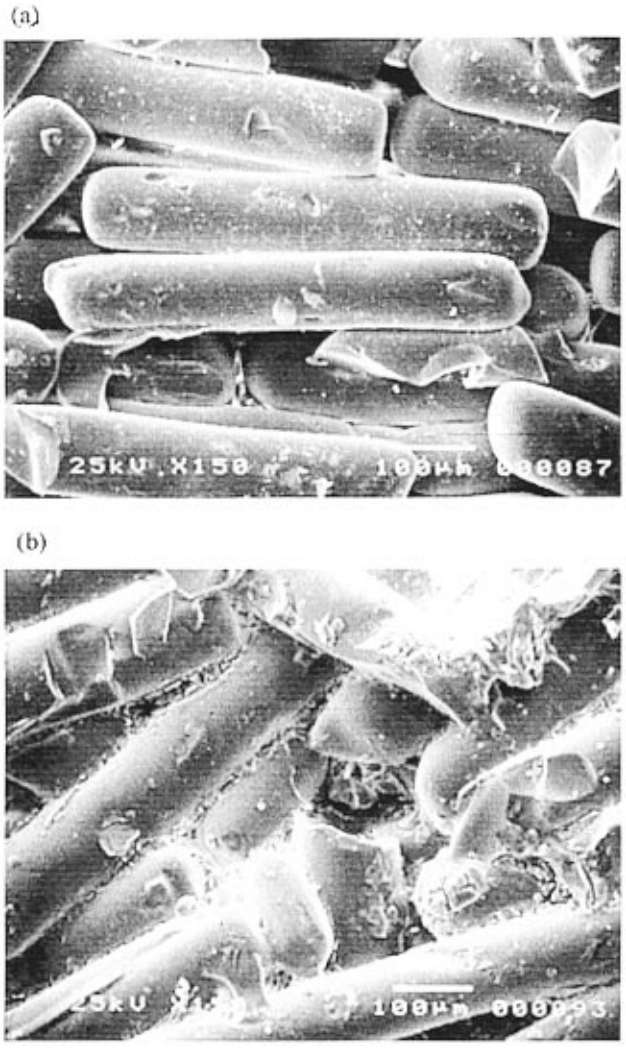

Figure 26. SEM image of glass filter (a) before and (b) after infiltration with MEA−alumoxane and firing at 290 °C for 2 h.

was accomplished with presinter heat treatment involving a controlled series of ramps and soaks (see Experimental Section). SEM images of the untreated frit (Figure 26a) and the frit after infiltration and firing (Figure 26b) show that the alumoxane has penetrated between the glass "rods" of the filter frit and thus decreased the remaining pore size. We are continuing our investigations into the use of the alumoxanes in the application of slip-coated filter membranes. The choice of alumoxane and firing conditions will be chosen to produce membranes with low density/high porosity.

Potential Environmental Impact of the Carboxylate−Alumoxanes. The proposed synthetic methodology would impact the release of contaminants to the environment on at least two distinct levels. First, the new synthetic methodology for producing these ceramic materials will eliminate the use of toxic solvents and reduce energy consumption, especially in the case of tape casting. With respect to the use of the carboxylate alumoxanes as binders in green body processes, byproducts formed from the combustion of plasticizers and traditional binders will be minimized, and with regard to sol−gel synthesis the use of acids may be eliminated. Thus, the process will reduce the potential for environmental release through the use of more environmentally benign feedstocks and an alternative synthetic procedure that will improve energy efficiency.

Second, due to the very versatile nature of the process, the proposed alumoxane process holds the potential for fabricating new ceramic nanofiltration and ultrafiltration membranes with enhanced specificity. Due to their stability during exposure to high temperatures and to organic solvents and oxidants, the ceramic membranes are particularly well suited for separations required in less environmentally benign industrial processes in which options for pollution prevention must focus on materials recovery and reuse in the absence of suitable alternative processes.

Finally, the alumoxane chemistry in solution may prove to be useful as a potentially new class of coagulants. These coagulants might be tailored by variation of the chain length of the organic substituents to optimize colloid destabilization, organic removal, or precipitation of metals in water, wastewater, and industrial waste treatment.

Conclusion

We have shown that the reaction of boehmite with carboxylic acids in water results in the formation of carboxylate−alumoxanes. The structure of the carboxylate alumoxane is best described as being an Al−O nanoparticle capped with carboxylate moieties. IR spectroscopy suggests that the carboxylate acts as a bridging ligand to two aluminum centers. The carboxylate alumoxanes are infinitely stable under ambient conditions[45] and may be readily processed in aqueous media. The polyether-substituted carboxylic acids provide uniform colloidal dispersions in water; acetic acid substituted alumoxanes prepared in water also form stable colloids. The most significant result of this study is the synthesis of acetate−alumoxanes from acetic acid. The acetate−alumoxane require no VOCs in its synthesis, is water soluble, and is readily converted to alumina >500 °C with a ceramic yield greater than 75%. The low cost (36 ¢ lb^{-1}) of acetic acid and low toxicity of its aqueous solutions offers an entry into a high ceramic yield, environmentally benign, ceramic precursor system.

Pyrolysis of the carboxylate−alumoxane yields alumina with low carbon contamination. The ceramic yield and the resulting physical properties of the alumina thus formed are dependent on the organic substituent. The acetate derivative A−alumoxane gives the highest ceramic yield and allows for the formation of alumina bodies. In addition to being processable preceramic materials, the aqueous processability of the carboxylate−alumoxanes allows for their use as the binder in traditional ceramic "green body" processing. The nanoparticle size of the carboxylate alumoxanes allows for full infiltration into microporous substrates which upon pyrolysis and sintering offers a method for their use as chemical infiltration and surface repair agents.

(45) At high pH (>9) it appears that the carboxylate ligands can be stripped off, i.e., after treatment with NaOH solution, the ceramic yield of MEA−alumoxane increases from 27% to 85%.

Experimental Section

Research grade pseudo-boehmite (100%) was kindly provided by Vista Chemical Co. All carboxylic acids were obtained commercially (Aldrich) and were used as received. Melting points and thermogravimetric/differential thermal analyses were obtained on a Seiko 200 TG/DTA instrument using a carrier gas of dry nitrogen, air, or oxygen. Infrared spectra (4000−400 cm^{-1}) were obtained using Nicolet 760 and Perkin-Elmer 1600 Series spectrometers, as Nujol mulls on KBr plates. Solution ^{1}H, ^{13}C, and ^{27}Al NMR spectra were obtained on either Bruker AM-250 and Bruker AM-300 spectrometers. Chemical shifts are reported relative to $SiMe_4$ (external), $[Al(H_2O)_6]^{3+}$ (external), or $CDCl_3$ (solvent) unless otherwise stated. UV−visible spectra were obtained on a Shimadzu UV-1601 spectrophotometer. Photon correlation spectra were obtained using a Malvern Automeasure 4700 V4 spectrometer. Additional particle size analyses were obtained using a Coulter LS230 particle size analyzer. Gel permeation chromatography data were obtained on a Shodex instrument utilizing a Waters HPLC. Surface area measurements were obtained utilizing a BET Model 4203 gas desorption instrument on samples dried for 12 h at 110 °C and then degassed in helium for 2 h at 110 °C. To enable XRD analysis, powder samples were mounted on glass slides prior to analysis. Data were collected on a Siemens D5000 diffractometer. SEM studies were performed on a JEOL JSM-5300 scanning microscope. A small amount of the as-synthesized material was attached to an aluminum stub with graphite paint. Due to the insulating nature of the materials, focusing and visual examination was problematical. Therefore, in some cases a thin layer of gold was sputtered onto the sample to provide a conducting surface. Transmission electron microscopy was conducted on a JEOL 2010 transmission electron microscope operated at 200 kV. Samples were embedded in epoxy, and thin specimens were produced by standard thinning methods: specimens were polished to thicknesses below 100 μm, dimpled to less than 20 μm minimum thickness, and finally ion milled to electron transparency. Hardness data were measured using a Micromet Microindenter with a standard diamond tip. AFM measurements were made on a Nanoscope IIIa scanning probe microscopic controller (Digital Instruments). Probes were FESP supplied by Digital Instruments and were utilized in the tapping mode. The scan rate was 1 Hz, and the number of samples taken on the fast scan axis was 512 per line. Data are reported as height.

Synthesis of MEEA−Alumoxane. Pseudoboehmite (20.0 g, 334 mmol) and [(methoxyethoxy)ethoxy]acetic acid (102 mL, 668 mmol) were refluxed in water (400 mL) which resulted in a clear solution after 72 h. The solution was centrifuged at 6000 rpm for 1 h and decanted. Removal of the volatiles in vacuo (10^{-2} Torr) at 90 °C yielded a gel which was dissolved in ethanol (100 mL) while stirring (10 min) and then triturated with diethyl ether (200 mL). The white solid powder thus obtained was redissolved in water (100 mL) and dried at 50 °C for 24 h, resulting in a clear glassy material. The MEEA−alumoxane is soluble in water, methanol, chloroform, and methylene chloride. IR (Nujol, cm^{-1}) 3441 (s), 3298 (s), 3093 (m), 1608 (m), 1255 (m), 1070 (s), 789 (m), 732 (w), 625 (m), 481 (m). ^{1}H NMR (D_2O) δ 3.92 (2H, s, O_2CCH_2), 3.59 (6H, m, CH_2), 3.53 (2H, m, CH_2), 3.30 (3H, s, OCH_3). ^{13}C NMR (D_2O) δ 177.5 (O_2C), 70.9 (CH_2), 69.5 (CH_2CH_2), 69.3 (CH_2), 58 (CH_3). ^{27}Al NMR ($CDCl_3$) δ 6 ($W_{1/2}$ = 3500 Hz).

Synthesis of MEA−Alumoxane. Pseudoboehmite (10.0 g, 167 mmol) and (methoxyethoxy)acetic acid (38.0 mL, 333 mmol) were refluxed in water (100 mL) for 24 h, resulting in a clear solution. The solution was centrifuged at 6000 rpm for 1 h and decanted. The water was removed in vacuo (10^{-2} Torr) at 50 °C, resulting in a gel. The gel was washed with Et_2O (3 × 75 mL) and then dissolved in EtOH (50 mL) while stirring (10 min). The MEA−alumoxane was precipitated via the addition of Et_2O (100 mL) as a white powder. After drying overnight at 50 °C the solid yield was approximately 25 g. The MEA−alumoxane is soluble in H_2O, $CHCl_3$, and CH_2Cl_2. IR (Nujol, cm^{-1}) 3493 (s), 3303 (s), 3048 (w), 1649 (m), 1598 (m), 1260 (m), 1024 (w), 799 (m), 727 (w), 625 (m), 476 (m). ^{1}H NMR (D_2O) δ 3.90 (2H, s, O_2CCH_2), 3.56 (4H, m, CH_2), 3.28 (3H, s, OCH_3). ^{13}C NMR (D_2O) δ 178.2 (O_2C), 75.6 (CH_2), 74.1 (CH_2), 73.9(CH_2), 62.6 (CH_3). ^{27}Al NMR ($CDCl_3$) δ 6 ($W_{1/2}$ = 3800 Hz).

Synthesis of MA−Alumoxane. Pseudoboehmite (10.0 g, 167 mmol) and methoxyacetic acid (25.6 mL, 334 mmol) were refluxed in water (150 mL) for 24 h, which resulted in a white cloudy solution with a trace of insoluble particles. The water was removed in vacuo (10^{-2} Torr) at 50 °C resulting in a white powder which was washed with Et_2O (4 × 150 mL) and then dissolved in ethanol (100 mL) while stirring (50 min). The alumoxane was precipitated via the addition of ether (300 mL). After drying overnight at 50 °C the solid yield was approximately 20 g. The powder was dissolved in water (100 mL), isolated by filtration, concentrated under vacuum, and dried at 50 °C, resulting in a white solid material. The MA−alumoxane is soluble in water, chloroform, and methylene chloride. IR (Nujol, cm^{-1}) 3446 (s), 3288 (s), 1618 (s), 1332 (m), 1193 (w), 1137 (s), 1065 (m), 917 (m), 722 (s), 640 (m), 481 (m). ^{1}H NMR (D_2O) δ 3.89 (2H, s, O_2CCH_2), 3.35 (3H, s, OCH_3).

Synthesis of A−Alumoxane. Pseudoboehmite (20.0 g, 333 mmol) was slowly added to a vigorously stirring mixture of acetic acid (51.0 mL, 667 mmol) in water (200 mL). The resulting slurry was decanted after 10 min and then centrifuged at 6000 rpm for 1 h to yield a clear viscous solution. Removal of the volatiles in vacuo (10^{-2} Torr) at 90 °C results in clear, white granules. The granules were dissolved in water and dried for 24 h at 80 °C to yield a clear glassy material. The acetate−alumoxane is soluble in water and slightly soluble in ethanol. IR (Nujol, cm^{-1}) 3583 (w), 3298 (s), 3088 (s), 2089 (m), 1608 (m), 1557 (m), 1260 (m), 1070 (s), 799 (m), 737 (w), 625 (m), 487 (m). ^{1}H NMR (D_2O) δ 1.95 (2H, s, O_2CCH_3).

Synthesis of Aluminum Oxides. The synthesis of alumina is given below.

Method 1. The alumoxane (5.0 g) was heated to 500 °C for 2 h.

Method 2. The alumoxane (5.0 g) was heated to 500 °C for 2 h, and then the temperature was increased (5 °C/min) to a maximum temperature of 1000 °C which was then maintained for 2 h.

Fabrication of Alumoxane Green Bodies. A warm 70 wt % solution of MEEA−alumoxane (60 g) in water was blended in a 2:1 ratio with alumina powder (30 g). This material was then cast into a wax mold of a bolt head. After drying at room temperature, the wax mold is melted off and the green body set by drying at 120 °C for 2 h. The green body was then fired at 1000 °C for 16 h.

Infiltration Experiments: Cellulose Filter. A portion of a commercial cellulose fuel filter (NAPA) was placed in a pressure vessel under vacuum for minimum of 1 h. An aqueous solution of 8 wt % MEEA−alumoxane was added to the vessel such that the filter was completely immersed. The pressure vessel was opened, and the filter was placed in a drying oven for 20 min. This procedure was repeated two more times. After the final coating the filter was placed in an oven and heated to 120 °C for 2 h and then 1000 °C for 2 h. The temperature ramp was 30 °C h^{-1}.

Infiltration Experiments: Glass Filter Frit. As a further example, a coarse glass filter frit (pore size "C", 25−50 μm maximum pore diameter range) was placed in a Schlenk flask and evacuated (1 Torr) for 10 min. An aqueous solution of 10 wt % MEA−alumoxane was added through a rubber septum such that the frit was completely immersed. The frit was removed from the Schlenk and placed in a drying oven (80 °C) for 10 min. The infiltration was repeated. The frit was then placed in a tube furnace for heat treatment consisting of the following controlled series of ramps and soaks: ramp to 180 °C for at 2 °C min^{-1} and then soaked at that temperature for 90 min; ramp to 290 °C at 2 °C min^{-1} and then soak for an additional 120 min.

Acknowledgment. Financial support for this work was provided jointly by the Environmental Protection Agency and the National Science Foundation under the Technology for a Sustainable Environment Program (DMI9613068) and in part by the National Aeronatics and Space Administration under NRA 96-LeRC-1 Technology for Advanced High Temperature Gas Turbine Engines, HITEMP Program.

CM9703684